

Article

Optimal Dispatch of Regional Integrated Energy System Group including Power to Gas Based on Energy Hub

Zhilin Lyu ^{1,*} , Quan Liu ¹ , Bin Liu ¹ , Lijun Zheng ², Jiaqi Yi ¹ and Yongfa Lai ¹¹ College of Electrical Engineering, Guangxi University, Nanning 530004, China² State Grid Zhangjiajie Power Supply Company, Zhangjiajie 427000, China

* Correspondence: lyuzhilin@gxu.edu.cn

Abstract: Different renewable energy resources and energy demands between parks lead to waste of resources and frequent interactions between the regional distribution grid and the larger grid. Hence, an optimal dispatching scheme of the regional integrated energy system group (RIESG), which combines the power-to-gas (P2G) and inter-park electric energy mutual aid, is proposed in this paper to solve this problem. Firstly, for the park integrated energy system (PIES) with various structures, the coupling matrix is used to describe the input-output relationship and coupling form of multiple energy sources in the energy-hub (EH), which linearizes the complex multi-energy coupled system and is more conducive to the solution of the model. Secondly, the electrical coupling relationship of the system is improved by adding P2G to enhance the system's ability to consume renewable energy. Moreover, the installation cost of P2G is introduced to comprehensively consider the impact of the economic efficiency on the system. Finally, to minimize the network loss of energy flow, the optimal dispatching model of RIESG with P2G conversion is constructed through the electric energy mutual aid among the parks. The simulation shows that compared with the independent operation of each park's integrated energy system (IES), the proposed optimal dispatching strategy of RIESG achieves the mutual benefit of electric energy among park groups, reduces the dependency on the large power grid, and effectively improves the economy of system groups. In this condition, the renewable energy consumption rate reaches 99.59%, the utilization rate of P2G increases to 94.28%, and the total system cost is reduced by 34.83%.

Keywords: energy hub; coupling matrix; power to gas; regional integrated energy system group; electric energy mutual aid; renewable energy consumption



Citation: Lyu, Z.; Liu, Q.; Liu, B.; Zheng, L.; Yi, J.; Lai, Y. Optimal Dispatch of Regional Integrated Energy System Group including Power to Gas Based on Energy Hub. *Energies* **2022**, *15*, 9401. <https://doi.org/10.3390/en15249401>

Academic Editor: Alan Brent

Received: 11 November 2022

Accepted: 5 December 2022

Published: 12 December 2022

Publisher's Note: MDPI stays neutral with regard to jurisdictional claims in published maps and institutional affiliations.



Copyright: © 2022 by the authors. Licensee MDPI, Basel, Switzerland. This article is an open access article distributed under the terms and conditions of the Creative Commons Attribution (CC BY) license (<https://creativecommons.org/licenses/by/4.0/>).

1. Introduction

Today, green and efficient is the mainstream direction of energy development. Although the integrated energy system (IES), which can coordinate and optimize the dispatch of multiple energy sources, improve the efficiency of energy utilization, and promote the consumption of renewable energy has been vigorously developed, it also brings some difficulties and challenges [1], at the same time.

Since people are no longer satisfied with a single type of energy supply, and the energy demand is developing toward diversification, IES is becoming more and more complex, with different available types of renewable energy supply systems. For IES with complex multi-energy coupling, Zeng et al. [2] proposed a typical physical architecture of IES and mathematical modeling of various types of devices. However, the separate modeling of electric, thermal, and gas systems and components is challenging to represent the multi-energy coupling in a unified way, and there are knowledge barriers between different disciplines. For this reason, some scholars have proposed the unified energy path theory to unify the grid, heat, and gas network equations in mathematical form [3–7]. However, the unified energy path model is based on partial differential equations for analytical derivation, which is difficult to model and computationally intensive. In addition to the unified energy

path theory, there are also modeling approaches based on the energy hub (EH) for unified modeling. The concept of EH was first proposed in [8], and then the standardized matrix modeling method based on EH was proposed in [9]. Tianhao et al. [10] proposed the standardized multi-step modeling method and the linearized optimization method. The modeling method based on EH can describe various energy conversion relationships of IES using coupling matrices, but it has not been well applied in complex IES.

Moreover, there are momentary distribution characteristics of renewable energy output, such as the curve of solar power generation, which is the “hump” type, and the curve of wind power generation, which is the “saddle” type. Additionally, inadequate system peaking capacity will lead to many energy abandonment phenomena, improving the peaking capacity to enhance the flexibility of the IES. Therefore, scholars from various countries have conducted a lot of research around different energy storage methods for optimal system dispatch [11–15]. In the literature [11–13], heat and cold storage is carried out through combined heat and cold power generation, in [14], pumped hydro energy storage is carried out through reservoirs, and in [15], battery storage is carried out through vehicle to grid systems, for the optimal dispatch of renewable energy systems. The development of power to gas (P2G) technology can convert electrical energy, which is difficult to store in large quantities, into gas energy, which is easy to store and can consume more renewable energy, which falls in line with the concept of green energy development [16–20]. For the application of P2G technology, Cui et al. [21] introduced a two-stage operation of P2G to optimize the thermoelectric coupling and improve the energy utilization of the system. Liu et al. [22] applied the P2G technology to an integrated electric cooling and heating energy system to improve the renewable energy consumption capacity of the system. Lili et al. [23] used the P2G technology to convert excess renewable energy generation into methane as storage to reduce the system’s uncertainty risk caused by intermittent wind and solar energy. Although the positive effects of P2G on the system are reflected in the above studies, there is a common problem. In fact, only the economic benefits of P2G consumption on system operating costs are considered, while the impact of equipment installation costs on system economics is neglected, resulting in a large installed capacity and low overall utilization of P2G equipment. In the literature [21,22], the P2G equipment only operates at a high load during certain hours of the night and does not work most of the time, showing the “tip” characteristic. In [23], the P2G equipment works during the daytime and hardly works at night, showing the “peak” characteristic. This operating characteristic is determined by combining renewable energy output within the IES and customer energy demand.

With the further development of IES, there will be multiple parks integrated energy systems (PIESs) with different attributes in the same regional distribution system, forming a regional integrated energy system group (RIESG). Each park’s renewable energy resources and energy demand vary, resulting in a shortage or surplus of renewable energy generation capacity in the system. In order to ensure the energy demand of users, parks with insufficient power supply require purchasing power from the grid to make up for the shortage. For parks with a surplus power supply, some of them meet the grid connection conditions and sell power to the grid, which leads to frequent power sales to the grid and affects the stable operation of the grid. As the renewable energy, which is disconnected from the grid, cannot be consumed, resources are wasted. For the study of RIESG, Li et al. [24] proposed an optimal scheduling strategy, based on the demand response and master-slave game, which improves the overall economy of the system, and considers the competitive relationship among the parks without considering the cooperative relationship of each park in the region, and fails to reflect the advantages of RIESG scheduling. Luo et al. [25] proposed an optimization model based on the cooperative game, which mainly solves the problem of renewable energy volatility. However, the IES structure is the same in each park, which cannot reflect the existing differences in different parks. Zhou et al. [26] carried out differentiated modeling for different regional energy use attributes. It uses the park’s electric energy interaction as well as storage power plants to regulate wind power, which

helps improve the system's consumption capacity. However, the system only considered a single wind power generation without considering the diversified development status of renewable energy in each park.

According to the above problems and the current status of research, this paper proposes an optimal dispatching scheme for an integrated energy system group, with P2G conversion. This scheme integrates EH with the positive effects of P2G conversion technology and electric energy interaction among multiple parks integrated energy systems, on the economic operation of the system group, and constructs a RIESG with a weak dependence on large power grids and strong renewable energy consumption capacity. The main contributions in this paper are as follows:

1. Extending the modeling method, based on the graph theory and coupling matrix, to a RIESG with P2G conversion that enables efficient and flexible differentiated modeling of each PIES. In this method, the linear coupling matrix is used to describe the energy conversion relationship of each energy component, with each branch energy flow as a variable, which can portray the dynamic process and coupling relationship of energy flow within the system, and balance the accuracy of the model with the complexity of the problem, which is beneficial to the solution of the optimal dispatching model of the energy system cluster.
2. The optimal dispatching strategy combining P2G, and inter-park power mutual aid is proposed, using P2G equipment to enhance the park's renewable energy consumption capacity. In this way, power complementarity is used to balance the resources of each park, combine the two to solve the frequent interaction problem between the distribution network and the power grid in the same region, and reduce the installed capacity of P2G equipment together with improving the utilization rate of P2G equipment, while ensuring the consumption of renewable energy. Thus, the operation economy of the RIESG is comprehensively improved.

2. Construction of EH Model

The concept of EH and modular modeling contribute to the optimal analysis of multi-energy coupled systems [8–10]. Therefore, this paper applies graph theory and coupling matrix modeling approaches to specific IES in order to meet the need for differentiated modeling of EH in different parks.

2.1. Modeling Method

The structure of the EH from the graph theory perspective is shown in Figure 1. The standardized coupling matrix modeling of the EH can be performed by analogy to the power system matrix modeling approach. The EH uses branches to represent the energy flow in the EH, nodes to represent the energy conversion and storage devices, and ports to define the input and output of the energy conversion and storage devices.

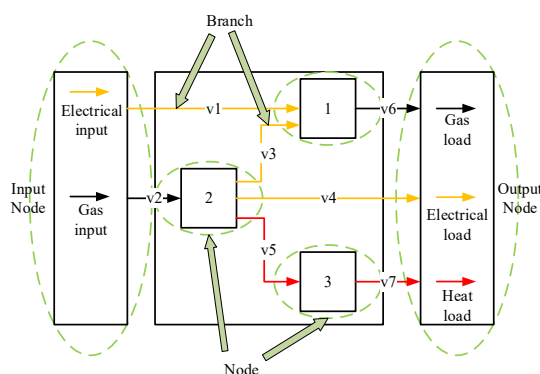


Figure 1. A graph theory perspective of EH.

For a node in an EH, a node port-branch correlation matrix A can be defined. The number of rows in the matrix is equal to the sum of the input and output port types of the node’s transformation device, and the number of columns is equal to the number of branches of the entire system. The elements of matrix A are 1, if a branch is connected to the node’s input port, -1 , if it is connected to the node’s output port, and 0, if it is not connected to any node’s port.

$$H_{ij} = \begin{matrix} & \begin{matrix} V_{in.1} & V_{in.2} & \cdots & V_{in.a} & V_{out.1} & \cdots & V_{out.b} \end{matrix} \\ \left[\begin{array}{ccccccc} \eta_{in.1-out.1} & 0 & 0 & 0 & 1 & 0 & 0 \\ \vdots & 0 & 0 & 0 & 0 & \ddots & 0 \\ \eta_{in.1-out.b} & 0 & 0 & 0 & 0 & 0 & 1 \\ 0 & \eta_{in.2-out.1} & 0 & 0 & 1 & 0 & 0 \\ 0 & \vdots & 0 & 0 & 0 & \ddots & 0 \\ 0 & \eta_{in.2-out.b} & 0 & 0 & 0 & 0 & 1 \\ 0 & 0 & \ddots & 0 & 0 & \vdots & 0 \\ 0 & 0 & 0 & \eta_{in.a-out.1} & 1 & 0 & 0 \\ 0 & 0 & 0 & \vdots & 0 & \ddots & 0 \\ 0 & 0 & 0 & \eta_{in.a-out.b} & 0 & 0 & 1 \end{array} \right] & \left[\begin{array}{l} V_{in.1} \rightarrow V_{out.1} \\ \vdots \\ V_{in.1} \rightarrow V_{out.b} \\ V_{in.2} \rightarrow V_{out.1} \\ \vdots \\ V_{in.2} \rightarrow V_{out.b} \\ \vdots \\ V_{in.a} \rightarrow V_{out.1} \\ \vdots \\ V_{in.a} \rightarrow V_{out.b} \end{array} \right] \end{matrix} \quad (1)$$

For a conversion module with the a type of inputs and the b type of outputs, the node-port conversion characteristic matrix H_{ij} can be defined. Its rows $i = a * b$, are numerically equal to the input port category multiplied by the output port category, the physical meaning of which is the category of energy conversion between the input and output ports. Its column number, $j = a + b$, is equal to the sum of the input port type and output port type of the transformed device at that node. The different conversion efficiencies $\eta_{in.x-out.y}$ corresponding to different energy inputs and outputs is the value of the element of the column in which the input port is located relative to the row in which the conversion process ($V_{in.x} \rightarrow V_{out.y}$) is located. And the value of the element corresponding to the output port of this conversion process is 1, and the value of the rest of the elements is 0.

The node-branch energy conversion matrix Z , which uses the branched energy flow to describe the energy conversion relationship of the component, is the product of the node-port conversion characteristic matrix H and the port-branch correlation matrix A , as given in the following equation.

$$Z = HA \quad (2)$$

Considering the analogy with Kirchhoff’s current law for power system modeling, the energy conversion equation corresponding to the internal EH is:

$$ZV = 0 \quad (3)$$

where V is the branch energy flow variable.

For the input and output ports of the whole EH, the input and output port-branch correlation matrices are defined as X and Y , respectively. The number of rows in matrix X is equal to the number of input port energy types, and elements corresponding to the input branch is 1, and the rest is 0. Similarly, the number of rows in matrix Y is equal to the number of output port energy types, and the elements corresponding to the output branch is 1, and the rest is 0. The number of columns in both matrices is equal to the number of branches.

The integrated equations of the entire EH can be obtained by associating all components of the node-branch energy conversion matrices, as well as the input and output matrices, as follows:

$$\begin{bmatrix} X \\ Y \\ Z \end{bmatrix} V = \begin{bmatrix} V_{in} \\ V_{out} \\ 0 \end{bmatrix} \quad (4)$$

2.2. Modeling of Different Types of Nodes

According to the above modeling method, the equipment used in IES can be classified into conversion and energy storage types based on the energy conversion and storage characteristics. Moreover, the conversion type can be subdivided into single and multiple types based on the number of equipment conversion methods.

2.2.1. Single Conversion Type

The single conversion modeling takes P2G as an example, which equates the electrolysis of water and the methanation reaction included in the P2G technology to a single energy conversion module, to convert the electrical energy to gas energy with the structure shown as node 1, in Figure 1. The P2G efficiency is indicated by η_{P2G} .

The energy conversion category of node 1 is electrical energy to gas energy. Moreover, the input port type is electrical, and the output port type is gas. Therefore, the node-port conversion characteristic matrix of node 1 is:

$$H_1 = [\eta_{P2G} \quad 1] \quad (5)$$

The electrical input port of node 1 contains branches 1 and 3, the gas output port is branch 6, and the EH contains 7 branches. Thus, the port-branch correlation matrix of node 1 can be presented as follows:

$$A_1 = \begin{bmatrix} 1 & 0 & 1 & 0 & 0 & 0 & 0 \\ 0 & 0 & 0 & 0 & 0 & -1 & 0 \end{bmatrix} \quad (6)$$

The node-branch energy conversion matrix for node 1 is:

$$Z_1 = H_1 A_1 = [\eta_{P2G} \quad 0 \quad \eta_{P2G} \quad 0 \quad 0 \quad -1 \quad 0] \quad (7)$$

The EH branch column variables are:

$$V = \begin{bmatrix} v_1 \\ v_2 \\ v_3 \\ v_4 \\ v_5 \\ v_6 \\ v_7 \end{bmatrix} \quad (8)$$

The node 1 energy flow conversion equation can be expressed as:

$$Z_1 V = 0 \quad (9)$$

According to (5)–(9), the following equation can be obtained.

$$\eta_{P2G} v_1 + \eta_{P2G} v_3 = v_6 \quad (10)$$

This energy flow conversion equation satisfies the physical significance of P2G to convert electrical energy to gas energy with the conversion efficiency of η_{P2G} .

2.2.2. Multiple Conversion Type

Multiple conversion type modeling is exemplified by combined heat and power (CHP) units, and the CHP device structure is shown in node 2, in Figure 1. The energy conversion can be categorized as gas to electric energy and gas to heat energy. The input port type is gas, and the output port type is electric and heat. The efficiencies of electricity and heat productions are $\eta_{CHP,E}$ and $\eta_{CHP,H}$, respectively. Thus, the node-port conversion characteristic matrix of node 2 is:

$$H_2 = \begin{bmatrix} \eta_{CHP,E} & 1 & 0 \\ \eta_{CHP,H} & 0 & 1 \end{bmatrix} \quad (11)$$

The gas input port of node 2 is branch 2, the electrical output port includes branches 3 and 4, the thermal output port is branch 5, and the EH contains 7 branches. Thus, the port-branch correlation matrix of node 2 is:

$$A_2 = \begin{bmatrix} 0 & 1 & 0 & 0 & 0 & 0 & 0 \\ 0 & 0 & -1 & -1 & 0 & 0 & 0 \\ 0 & 0 & 0 & 0 & -1 & 0 & 0 \end{bmatrix} \quad (12)$$

The node-branch energy conversion matrix for node 2 is:

$$Z_2 = H_2 A_2 = \begin{bmatrix} 0 & \eta_{CHP,E} & -1 & -1 & 0 & 0 & 0 \\ 0 & \eta_{CHP,H} & 0 & 0 & -1 & 0 & 0 \end{bmatrix} \quad (13)$$

Combined with the EH branch column variables, the node 2 energy flow conversion equation can be expressed as:

$$Z_2 V = 0 \quad (14)$$

According to (11)–(14), the below equation is obtained:

$$\begin{cases} \eta_{CHP,E} v_2 = v_3 + v_4 \\ \eta_{CHP,H} v_2 = v_5 \end{cases} \quad (15)$$

This energy flow conversion equation satisfies the physical meaning of CHP, converting gas energy to electrical energy with conversion efficiency $\eta_{CHP,E}$, and gas energy to heat energy with conversion efficiency $\eta_{CHP,H}$.

2.2.3. Energy Storage Type

The heat storage device is an example of energy storage type device modeling, and its structure is shown as node 3, in Figure 1. The energy storage device is a special energy conversion and storage module which describes the input and output variables of the energy storage device. Furthermore, a dummy variable needs to be introduced to describe the change of energy inside the energy storage.

For the heat storage device represented by node 3, ΔE_h denotes the amount of heat storage change, $\eta_{HS,C}$ represents the charging efficiency, and $\eta_{HS,D}$ expresses the discharging efficiency. The node-port conversion characteristic matrix of node 3 can be written as:

$$H_3 = [\eta_{HS,C} \quad 1/\eta_{HS,D} \quad 1] \quad (16)$$

In node 3, the heat input port is branch 5, the heat output port is branch 7, and the dummy variable is ΔE_h . Therefore, the whole number of EH branches is 8, and the EH branch column variable is written after increasing and expanding as follows:

$$V' = \begin{bmatrix} v_1 \\ v_2 \\ v_3 \\ v_4 \\ v_5 \\ v_6 \\ v_7 \\ \Delta E_h \end{bmatrix} \quad (17)$$

The augmented port-branch correlation matrix for node 3 is:

$$A'_3 = \begin{bmatrix} 0 & 0 & 0 & 0 & 1 & 0 & 0 & 0 \\ 0 & 0 & 0 & 0 & 0 & 0 & -1 & 0 \\ 0 & 0 & 0 & 0 & 0 & 0 & 0 & -1 \end{bmatrix} \quad (18)$$

The node-branch energy conversion matrix for node 3 is:

$$Z'_3 = H_3 A'_3 = [0 \quad 0 \quad 0 \quad 0 \quad \eta_{HS,C} \quad 0 \quad -1/\eta_{HS,D} \quad -1] \quad (19)$$

Combined with the EH expansion branch column variables, the node 3 energy flow conversion equation can be expressed as:

$$Z'_3 V' = 0 \quad (20)$$

According to (16)–(20), the following equation is obtained.

$$\Delta E_h = \eta_{HS,C} v_5 - (1/\eta_{HS,D}) v_7 \quad (21)$$

The energy flow equation satisfies the basic charging and discharging characteristics of the energy storage device.

2.3. EH Overall Model

Figure 2 shows the EH structure of the PIES, containing single conversion type equipment: gas boiler (GB), electric cooling (EC), heat pump (HP), water absorption refrigerator group (WARG), and P2G; containing multiple conversion type equipment: CHP; containing energy storage type equipment: electricity storage (ES), heat storage (HS), cooling storage (CS), and gas storage (GS). According to the above modular modeling method in Figure 2, the energy conversion relationship matrix is presented in (22), and each park's energy conversion relationship matrix can be added and deleted based on the differences in energy conversion modules in each park.

implies energy loss cost; $\lambda_e, \lambda_g, \lambda_{solar}$, and λ_{wind} are electricity purchase price, gas purchase price, solar disposal price, and wind disposal price, respectively; $\lambda_{om,i}$ is the operation and maintenance coefficient of equipment i ; $P_e^{buy}(t), P_g^{buy}(t), P_i(t), P_{solar}^{loss}(t)$, and $P_{wind}^{loss}(t)$ are electricity purchase, gas purchase, the output power of equipment i , solar disposal power, and wind disposal power at time t , respectively.

To consider the economic benefits of adding P2G to PIES, the cost of P2G installation must be converted to each dispatch cycle to be included in the total system cost, and the cost of P2G equipment installation is obtained as:

$$C_{P2G}^{install} = \lambda_{P2G}^{install} P_{P2G}^{cap} \quad (24)$$

where $C_{P2G}^{install}$ denotes P2G installation cost, $\lambda_{P2G}^{install}$ represents P2G installation price conversion factor, and P_{P2G}^{cap} implies P2G installation capacity.

Therefore, the total cost of running the PIES installation C is:

$$C = C_{Op} + C_{P2G}^{install} \quad (25)$$

From (10), (15), and (21), it can be concluded that different types of modeled modules satisfy energy conservation. Moreover, the integrated EH Equations (4) and (22) composed of each module satisfy the power balance equation constraint, and the remaining inequality constraints are as follows.

Equipment power constraints:

$$P_{i,min} \leq P_i(t) \leq P_{i,max} \quad (26)$$

where $P_{i,max}$ and $P_{i,min}$ are the upper and lower limits of the output force of equipment i , respectively.

Energy storage element cycle energy storage constraint:

$$\begin{cases} SOC_{i,min} \leq SOC_i(t) \leq SOC_{i,max} \\ SOC_i(T) = SOC_i(0) \end{cases} \quad (27)$$

where $SOC_{i,max}$ and $SOC_{i,min}$ are the upper and lower limits of energy storage of device i , respectively. Moreover, $SOC_i(t)$ denotes the energy storage of each element at time t .

Climbing rate constraint:

$$|\Delta P_i| \leq P_{i,climb} \quad (28)$$

where ΔP_i and $P_{i,climb}$ denote the output variation and climbing rate of device i , respectively.

3. Optimal Scheduling of RIESG

A large amount of clean energy is underutilized in surplus power parks due to the differences in renewable energy resources and energy demand among PIES, and the limited regulation capacity of individual system optimization and dispatch. In contrast, power shortage parks require a regular power supply from large grids. Therefore, this paper proposes a complementary optimal dispatching model for RIESG with the electric energy interaction between each park as a link.

Firstly, wind and solar power generation and various types of load data of each park are input, and according to the renewable energy type and energy conversion module of each park, the energy branch decision variables are set in Matlab, using Yalmip toolbox. The integrated equations of each hub are obtained by modeling each type of node according to the modular modeling method of the energy hub. Using Equations (4) and (26)–(28) as the constraints and Equation (23) as the objective for each park to optimally dispatch itself, the Gurobi solver is invoked to solve for the surplus or shortage of electricity under optimal operation of each park. Then, the multi-node optimal flow model is constructed with the surplus park as the source node, the shortage park as the load node, and the surplus park that provides the most power as the balance node, with the minimum system network

loss as the objective function when the energy flow is mutual aid. The second-order cone relaxation technique is used to convert the mathematical model into a second-order cone programming problem, and the Gurobi solver is invoked to find the output power of each source node to obtain the optimal solution of energy mutual aid among the parks. The source node transmits power to the load node to achieve the effect of making full use of renewable energy in the surplus park, and reducing the dependence on the power grid in the shortage park, bringing into play the regulating ability of the system group and realizing complementary optimization in the region. Finally, according to the energy mutual aid results, the optimal scheduling scheme for each park is modified and obtained.

The flow chart for solving the optimal dispatching model of the RIESG is shown in Figure 3.

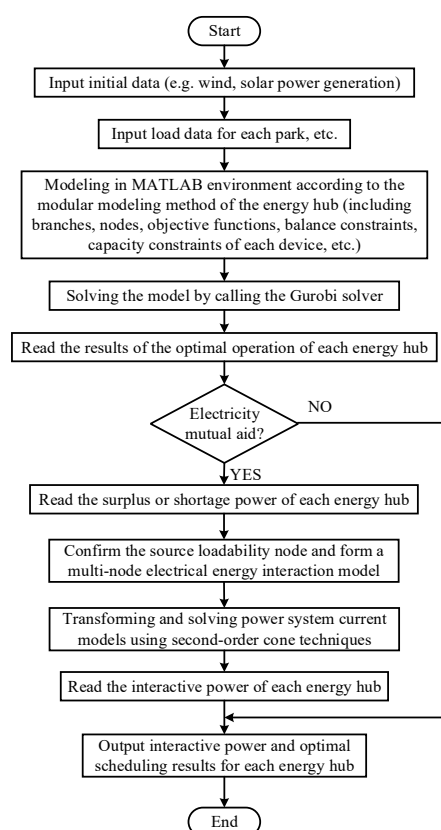


Figure 3. Flowchart for solving the optimal scheduling model of RIESG.

4. Simulation and Results

This chapter will verify the effectiveness and reasonableness of the proposed optimal dispatching strategy for the RIESG with P2G conversion through the analysis of case studies.

4.1. Case System

In this paper, four different IES structures for parks are constructed for resource and energy use differences, where $PIES_1$ is an IES of electricity, cooling, heat, and gas for parks with abundant wind and solar resources, $PIES_2$ and $PIES_3$ are integrated energy systems for parks with a single type of wind or solar energy, and $PIES_4$ is an IES for parks with complementary wind and solar energy. However, wind and solar energy resources are scarce compared with $PIES_1$, and the internal resources are inadequate to meet the load demand. The structural configuration of each PIES, renewable energy output, and various load demand curves are shown in Figures A1 and A2, in Appendix A. The proposed complementary topology of the RIESG is shown in Figure 4, and its line parameters refer to the standard data of IEEE 4 nodes system.

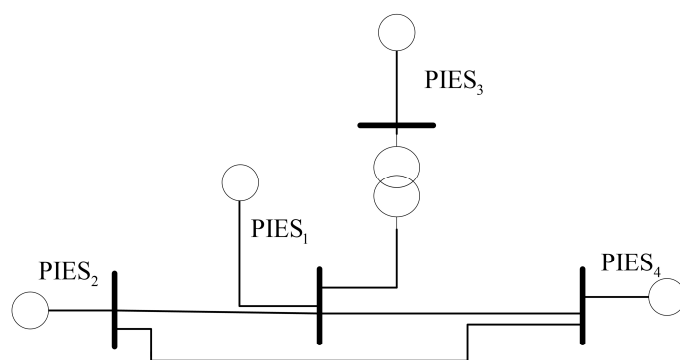


Figure 4. RIESG topology diagram.

The various parameters used for each system are adjusted based on [27–29], and the price of natural gas purchased by the system from the external gas grid is 2.65 RMB/m³, and the calorific value of natural gas is 9.88 (kWh)/m³. The price of sold electricity from the external grid of the system is a time-of-use tariff, and the energy price is shown in Figure 5.

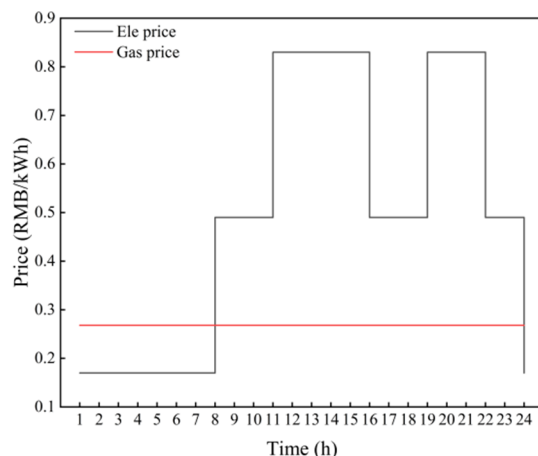


Figure 5. Energy price chart.

The operation and maintenance cost coefficients of each equipment are shown in Table 1, in which the abandoned energy cost is set to 150 RMB/MWh, and the converted cost of P2G equipment installation is 2500 RMB/MW. The simulation examples in this paper are programmed on the MATLAB software and modeled and solved using the YALMIP toolbox and Gurobi solver.

Table 1. Operation and maintenance cost factors for each equipment.

Equipment	Unit O&M Costs RMB/MWh
CHP	30
GB	20
EC	10
HP	10
WARG	25
ES	20
CS	20
HS	20
P2G	15
GS	20
Photovoltaic	80
Wind turbine	100

4.2. Case Scenario Setup

In this paper, 4 scenarios are considered for comparative analysis, including:

Scenario 1: Without considering the P2G equipment and the power interaction between parks, each park operates intending to optimize its economy. The utilization of renewable energy resources under the independent operation of each park is examined.

Scenario 2: Without considering the electric energy interaction between parks, but with considering the impact of P2G equipment on each park, the impact of adding different capacity P2G equipment on the economic operation of different parks is examined.

Scenario 3: Without considering the impact of P2G equipment on the economic operation of each park, but considering the electrical energy interaction between parks, the overall resource utilization of the RIESG operating mode is examined.

Scenario 4: Considering both P2G facilities and inter-park energy interactions, the impact of the complementary structure of a group of integrated regional energy systems containing P2G on each park is examined.

4.3. Results and Analysis

The energy flow of PIES can be obtained by solving each park in each scenario based on modular modeling of the EH. The solution time of scenario 4 is 0.0929 s, and the energy flow of PIES₁ is shown in Figure 6. The figure contains the energy flow values of each branch at each period, which visually reflects the energy flow process of each coupled component branch in the EH. The following further analysis is based on the energy flow diagram of each PIES in each scenario.

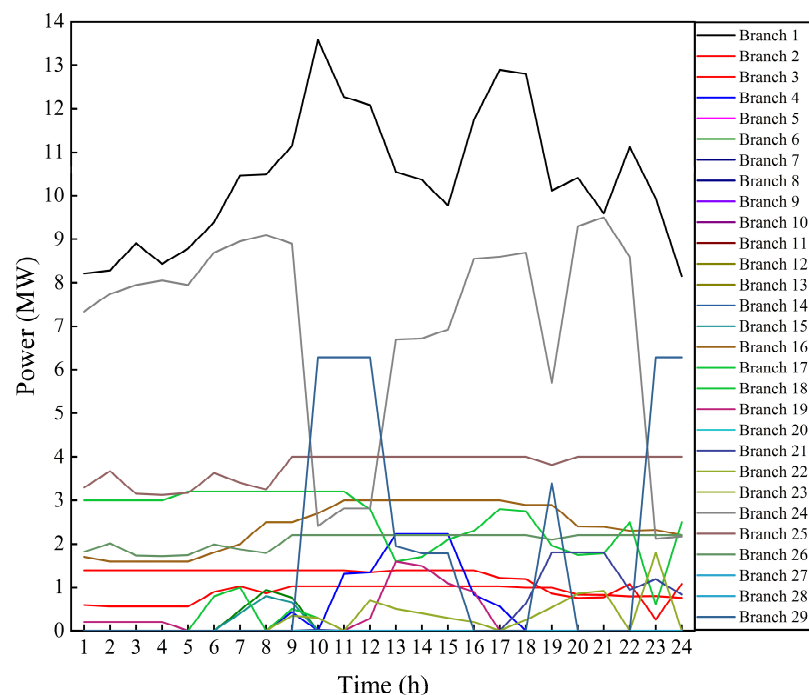


Figure 6. Energy flow of PIES₁ in scenario 4.

4.3.1. Scenario 1 Results Analysis

Each PIES under the scenario 1 setting operates independently to optimize its economy to meet the demand of various types of loads, and obtains the surplus power of each park, and the need for the external grid to provide power to cover the shortage, as shown in Figure 7.

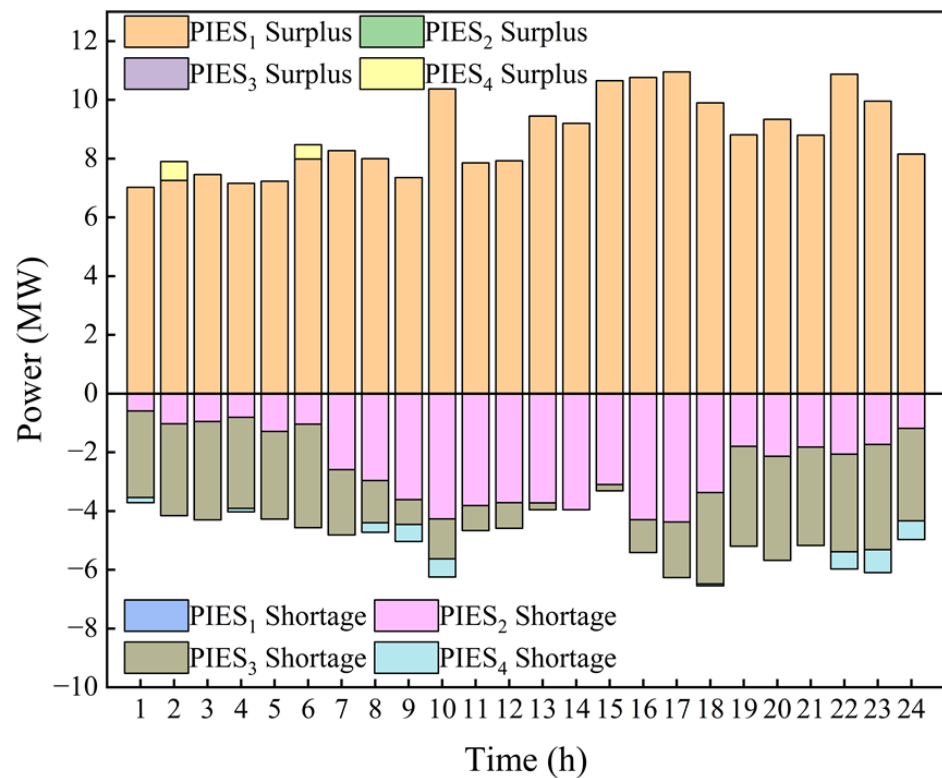


Figure 7. Power surplus and shortage of each PIES.

As can be seen in Figure 7, PIES₁ has a large surplus of renewable energy to meet its own load demand, due to the abundant wind and solar resources inside the park. It is worth noting that the surplus renewable energy cannot be consumed under the independent operation mode. PIES₂ is a single wind power generation system, and PIES₃ is a single photovoltaic power generation system. Since the renewable energy resources in the park are inadequate to supply the energy demand of the system itself, the situation reflects the time difference of scenery resources, in which PIES₂ is a wind power generation system, and the power shortage is larger in the daytime when the wind power generation is small, and PIES₃ is a photovoltaic power generation system, and the power shortage is larger at night. PIES₄ is a combination of wind and solar power generation systems. As the shortage of renewable energy resources in the park is still available, a small amount of external grid is required to cover up the shortage several times, and occasionally a small amount of surplus is not utilized. The results of the independent operation of the four PIESs reflect the resource and demand differences between the parks, and the region has the feasibility of inter-park energy mutual aid to achieve the complementarity of a RIESG.

4.3.2. Scenario 2 Results Analysis

According to the setting of scenario 2, each PIES is added with different electric to gas equipment capacities for optimized operation. The structure of PIES after adding the P2G equipment is shown in Figure 2 (taking PIES₁ as an example).

Since PIES₂ and PIES₃ have no unconsumed renewable energy in the park, no additional electricity to gas equipment is installed. PIES₄ has unconsumed renewable energy, but the unconsumed amount is small. Therefore, 1 MW of electricity to gas equipment is added, and the P2G equipment works as shown in Figure 8. The equipment only works at 2:00 and 6:00, which is a very low utilization rate for the P2G equipment.

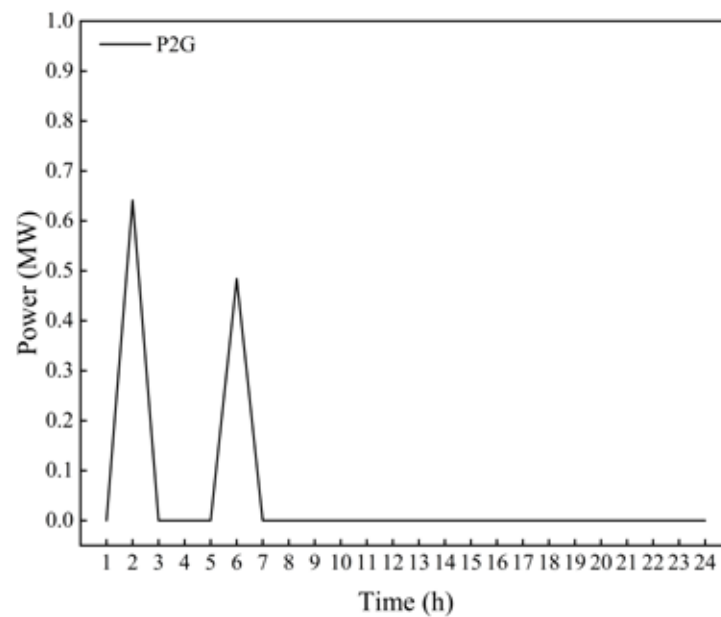


Figure 8. PIES₄ P2G facility consumption.

The operating cost of PIES₁, the total cost of installation and operation, and the renewable energy consumption of the system by installing different capacities of P2G equipment are shown in Figure 9. As can be seen, PIES₁ has a large amount of surplus power, which requires installing additional larger capacity P2G equipment for renewable energy consumption.

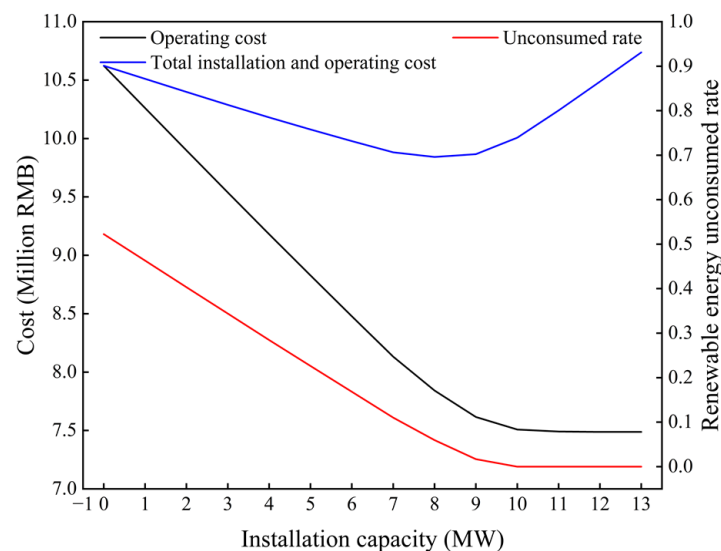


Figure 9. Cost and consumption of PIES₁ with different installed P2G capacities in Scenario 2.

It can be seen from Figure 9 that the larger the installed P2G capacity, the lower the unconsumed rate and the lower the operating cost, and the operating cost no longer decreases when the capacity reaches 12 MW. However, when the P2G capacity is greater than 8 MW, the equipment installation cost is greater than the economic benefit of the equipment to the system operation. Hence, the total system installation and operation cost increases. The equipment capacity with the lowest operating cost and total installation and operation cost is selected for further analysis. The equipment utilization and system consumption are shown in Figure 10.

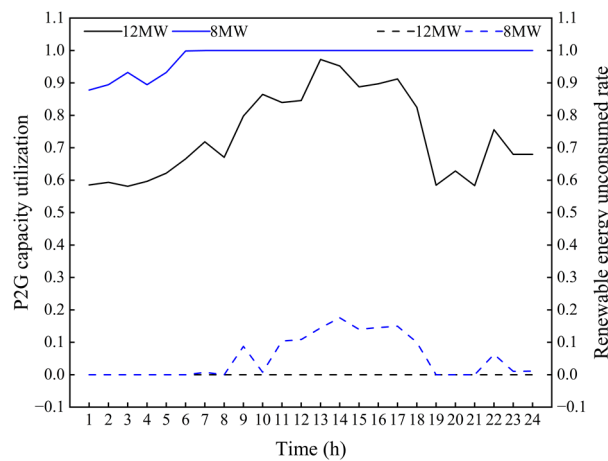


Figure 10. P2G utilization and dissipation in PIES₁ for scenario 2.

According to the operation results in Figure 10, a 12 MW P2G equipment can fully consume the renewable energy of PIES₁, but the utilization rate of the equipment only reaches 80% or more at time 10:00–18:00. The utilization rate of P2G equipment is above 90% when the capacity of P2G equipment is set to 8 MW, and the equipment operates at full load most of the time. However, it cannot fully consume renewable energy, and the unconsumed rate of renewable energy for the entire day is 5.95%, and the highest unconsumed rate reaches 17.57% at 14:00.

From the above results, it can be concluded that the installation of additional P2G equipment promotes the renewable energy consumption of PIES. However, for independently operated PIES, the utilization rate of P2G equipment and renewable energy consumption rate cannot be guaranteed simultaneously.

4.3.3. Scenario 3 Results Analysis

According to scenario 3, the inter-network electric energy interaction is carried out for the four PIESs, with the lowest network loss as the target function to realize the RIESG energy mutual aid, without requiring an external power grid for power shortage replenishment. Figure 11 illustrates the electric energy transmission and reception of each park, and the load demand diagram of PIES₁ before and after an interaction is shown in Figure 12.

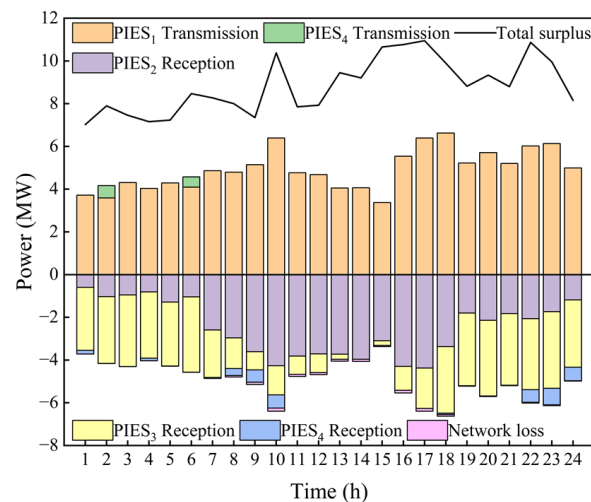


Figure 11. RIESG power interaction.

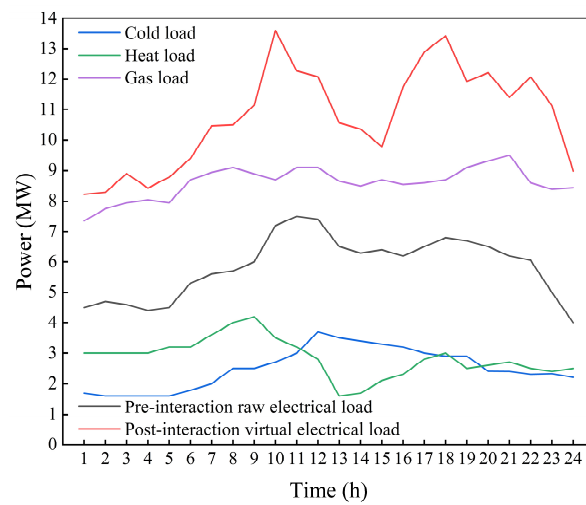


Figure 12. PIES₁ load demand diagram before and after interaction.

Comparing Figures 7 and 11, it can be seen that the complementary regional system transmits the surplus power in PIES₁ and PIES₄ to PIES₂ and PIES₃ for shortage replenishment. PIES₄ is able to consume the surplus power at 2:00 and 6:00, and the inter-park power interaction also covers the power shortage for the rest of the time. However, PIES₁ still has a large amount of unconsumed renewable energy after providing the power shortage in the rest of the parks, and the unconsumed power accounts for 30.03–68.30% of the surplus power before the interaction at each time. The above operation results and analysis prove that the interaction of multiple parks can play a complementary regional role and contribute to the overall renewable energy consumption. However, only relying on the form of mutual energy aid has a limited effect on the regional system, and cannot achieve the full consumption of renewable energy in the integrated energy system group.

4.3.4. Scenario 4 Results Analysis

Scenario 4 is the optimal dispatching scheme of RIESG considering P2G and park power interaction proposed in this paper. Based on scenario 3, additional P2G equipment is installed to further improve the capacity of PIES₁ to consume renewable energy.

Figure 13 shows the system cost curves of adding different capacities of P2G equipment at PIES₁ after the inter-campus power interaction and the consumption situation. As can be seen, when the capacity is 8 MW, the operation cost is the lowest and the lowest total system installation, and operation cost occurs when the capacity is 4 MW. These two nodes are selected for further analysis. The equipment utilization and system consumption are shown in Figure 14.

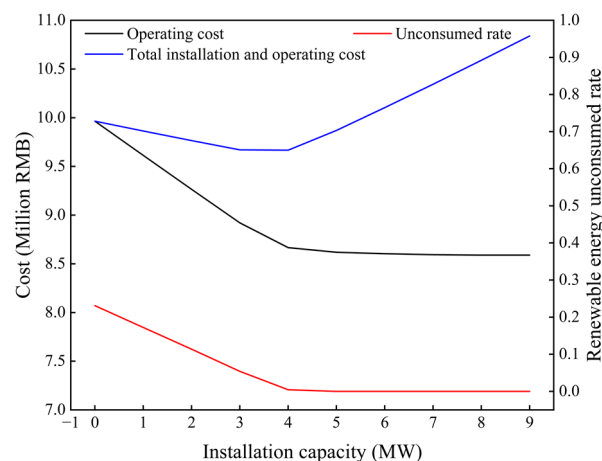


Figure 13. Cost and consumption of PIES₁ with different P2G capacities installed in Scenario 4.

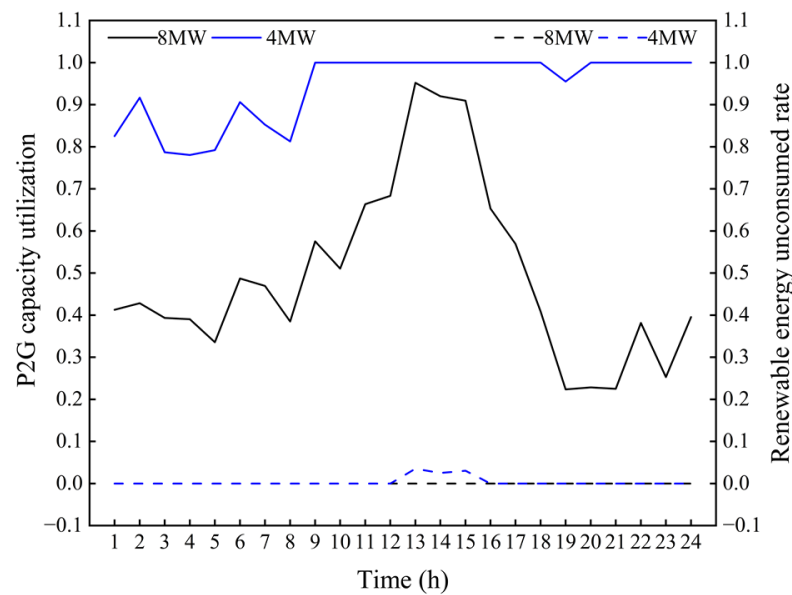


Figure 14. P2G utilization and dissipation in PIES₁ for scenario 4.

Compared with Scenario 2, the proposed solution in Scenario 4 consumes the surplus renewable energy in PIES₄ through the electric energy interaction between parks, and eliminates the additional P2G equipment installation in PIES₄. Moreover, it solves the problem of the “tip” of P2G equipment in PIES₄, as shown in Figure 8. It also turns the disadvantage of park electricity shortage in PIES₂ and PIES₃ into the advantage of regional electricity consumption, to relieve the consumption pressure of PIES₁ and significantly reduce the installed capacity of P2G equipment. In this paper, the installation of 4 MW of additional P2G equipment is chosen by considering the system economy and renewable energy consumption capacity. In this condition, the utilization rate of the equipment is more than 78%, and the average utilization rate reaches 94.28%, which solves the significant installed capacity requirement problem. Furthermore, the operation is “peak”, and the overall utilization rate is not high due to the cost of P2G installation in existing studies. The solution only has a small amount of unconsumed renewable energy between 13:00 and 15:00, the highest unconsumed rate is 3.51%, and the whole day unconsumed rate is 0.44%, which improves the equipment utilization rate and ensures the system’s consumption rate.

Scenario 4 adds 4 MW of P2G equipment and obtains the following results for the optimal dispatch of the RIESG.

In Figures 15–17, part of the surplus renewable energy of PIES₁ is used to make up the electric difference to other power shortage type parks, through the electric energy interaction of the parks within the region. Moreover, the other part is electrically coupled through the electric to gas equipment to meet part of the gas load demand. The optimal scheduling of RIESG can complement the advantages and disadvantages of each park within the region and fully use each park’s internal energy storage elements to maximize the economy of the RIESG. The total cost of each RIESG category consisting of four parks under each scenario is shown in Table 2.

From Table 2, the effect of P2G and regional complementarity on the economic operation of the RIESG can be analyzed. The results show that the P2G equipment mainly decreases the total system cost by reducing the gas purchase cost, and improving the renewable energy consumption capacity. Moreover, the complementary regional system mainly reduces the total system cost by declining the power purchase, energy disposal costs, and the capacity of power-to-gas equipment. In this situation, the total cost of system installation and operation of the proposed scheme is the lowest, at 34.83% lower than the total cost of independent operation of each park in Scenario 1.

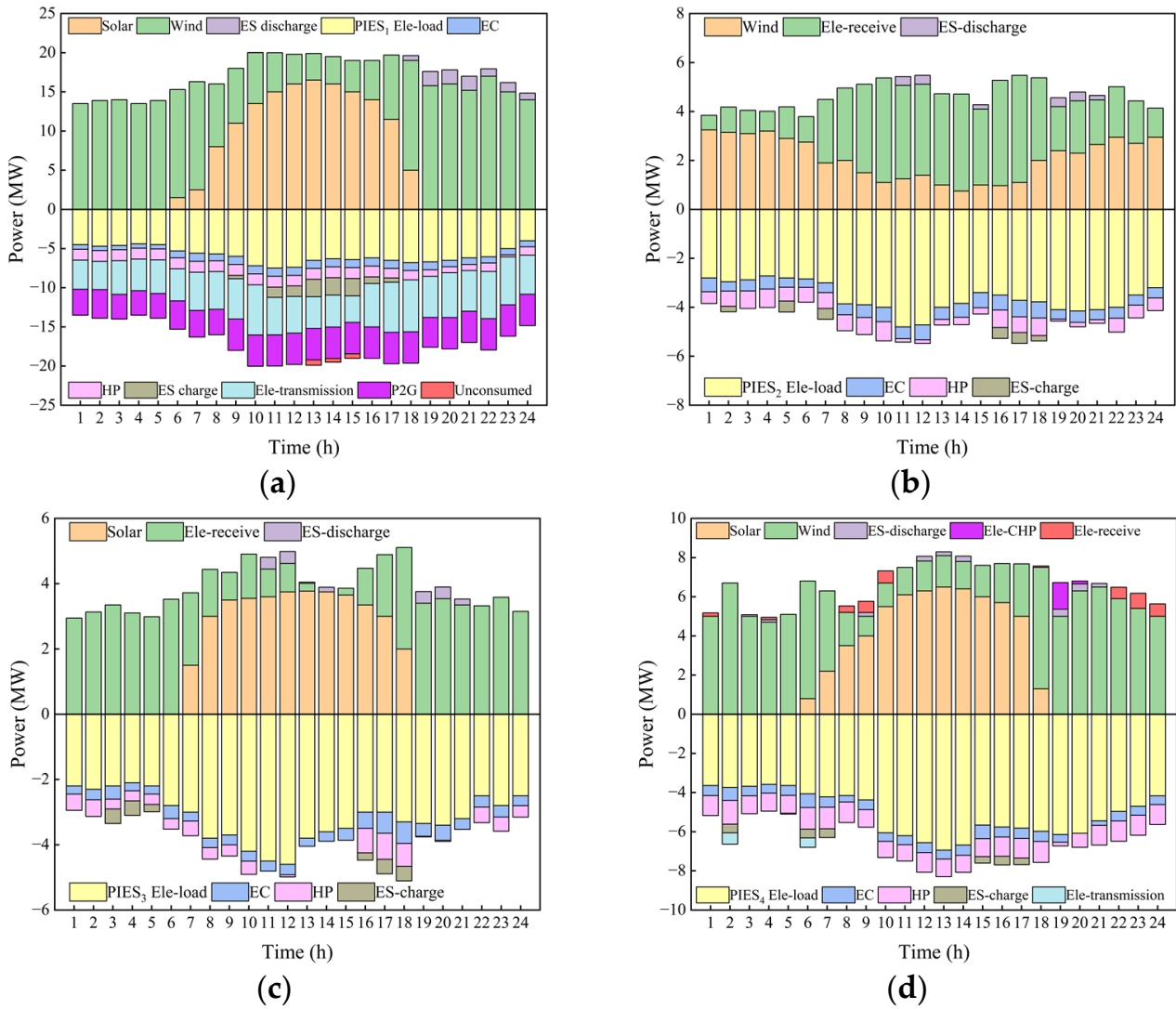


Figure 15. Electric network of each park of the RIESG: (a) PIES₁ electrical network; (b) PIES₂ electrical network; (c) PIES₃ electrical network; (d) PIES₄ electrical network.

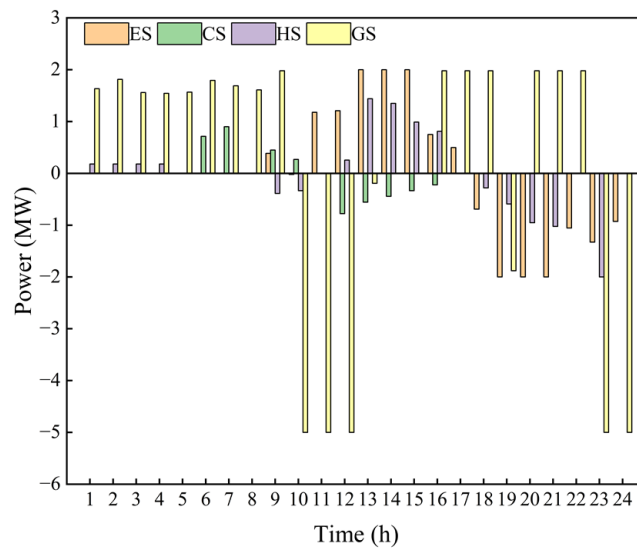


Figure 16. Scenario 4 PIES₁ various types of energy storage.

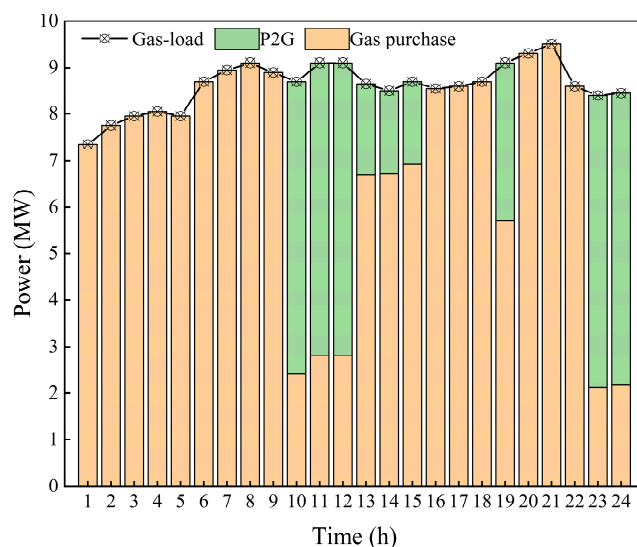


Figure 17. PIES₁ gas network for scenario 4.

Table 2. Costs of a RIESG under different scenarios.

Cost/RMB	Scene 1	Scene 2		Scene 3	Scene 4	
		12 MW *	8 MW *		8 MW *	4 MW *
C_{ele}	58,943	58,943	58,943	0	0	0
C_{gas}	62,599	37,049	39,987	62,595	51,273	51,789
C_{om}	43,361	69,172	66,183	54,525	66,068	66,057
C_{loss}	31,779	0	3601	14,035	63	327
C_{Op}	196,682	165,164	168,714	131,155	117,404	118,173
PIES ₁ $C_{P2G}^{install}$	0	30,000	20,000	0	20,000	10,000
PIES ₄ $C_{P2G}^{install}$	0	2500	2500	0	0	0
C	196,682	197,664	191,214	131,155	137,404	128,173

* PIES₁ installed P2G equipment capacity.

5. Conclusions

This paper establishes a RIESG optimization and dispatch model considering electricity to gas. The park complementarity is for a regionally integrated energy system consisting of several parks with different characteristics. The following conclusions are obtained by comparing and analyzing the optimization results of each park under different operation scenarios.

1. There are regional differences in renewable energy resources and structures within each park. This study applies the coupling matrix-based modeling method to a regional multi-park integrated energy system group to efficiently and flexibly model each PIES. At the same time, the method better describes the complex relationship of multi-energy coupling within the system, and intuitively reflects the flow of energy in the EH, while the flexible energy flow path provides more space for multi-energy collaboration.
2. The proposed optimal dispatch strategy of RIESG with P2G conversion helps improve the regional system's economy and reduce the dependence on the large grid. Compared with the independent operation of each park, the total cost is reduced by 34.83%. Through the electric energy interaction of each park, the surplus power of the surplus power type park is effectively utilized, and the shortage type park achieves full replenishment, which solves the frequent interaction with the large grid problem. The surplus renewable energy is consumed through P2G equipment, with a consumption rate of 99.59%.

Author Contributions: Conceptualization, Z.L.; methodology, Q.L.; software, Q.L., L.Z., J.Y. and Y.L.; validation, Z.L., Q.L. and B.L.; formal analysis, Q.L.; resources, Z.L.; data curation, Q.L. and L.Z.; writing—original draft preparation, Q.L.; writing—review and editing, Z.L., Q.L. and B.L.; visualization, J.Y. and Y.L.; supervision, Z.L. and B.L.; project administration, Z.L. and B.L. All authors have read and agreed to the published version of the manuscript.

Funding: This research was funded by the National Science Foundation of China (61364027) and the Natural Science Foundation of Guangxi (2019GXNSFAA185011).

Data Availability Statement: The data that support the findings of this study are available from the corresponding author upon reasonable request.

Conflicts of Interest: The authors declare that they have no known competing financial interest or personal relationships that could have appeared to influence the work reported in this paper.

Appendix A

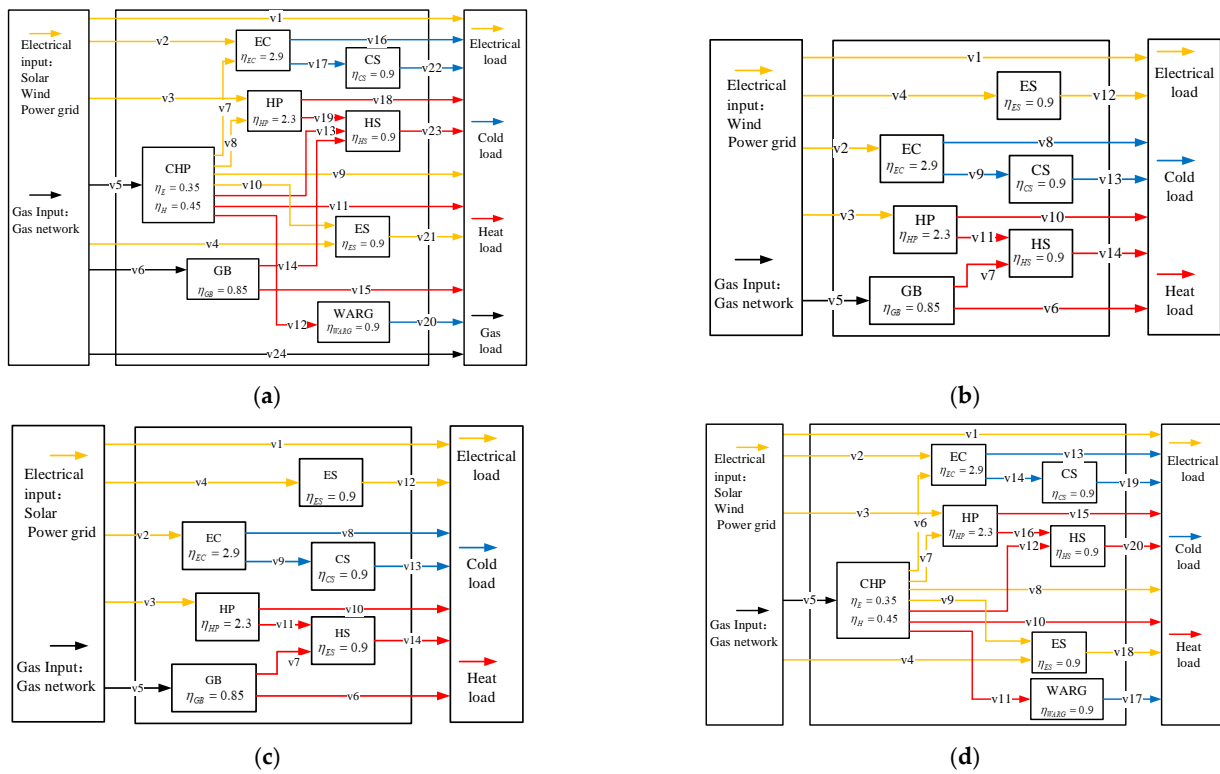


Figure A1. Structure configuration of each PIES: (a) PIES₁ structure configuration; (b) PIES₂ structure configuration; (c) PIES₃ structure configuration; (d) PIES₄ structure configuration.

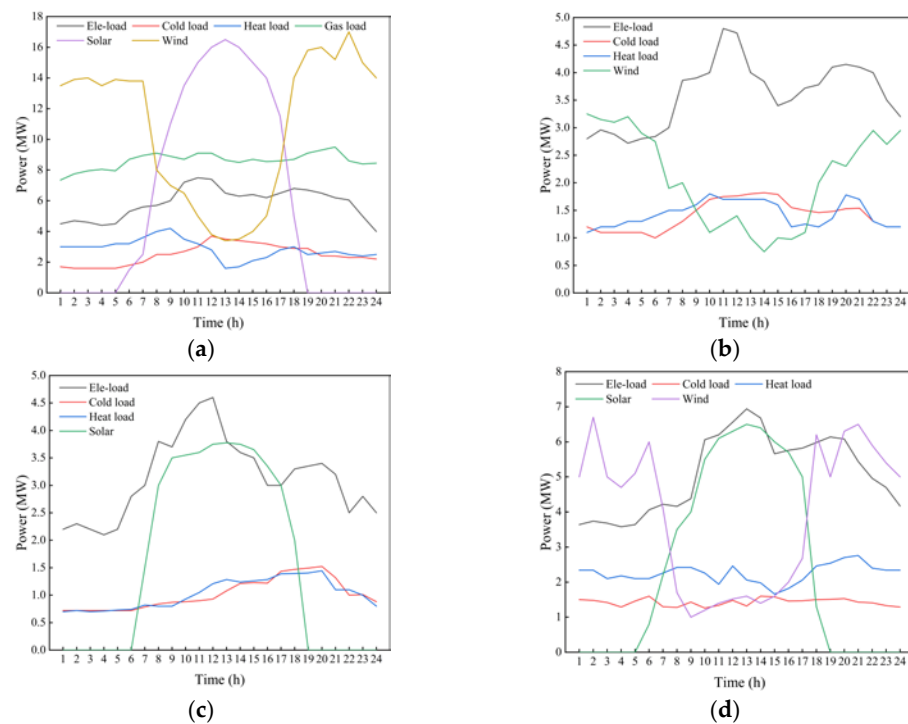


Figure A2. Renewable energy output and various load demand curves of each PIES: (a) PIES₁ renewable energy output and various load demand curves; (b) PIES₂ renewable energy output and various load demand curves; (c) PIES₃ renewable energy output and various load demand curves; (d) PIES₄ renewable energy output and various load demand curves.

References

- Li, J.; Zhu, M.; Lu, Y.; Huang, Y.; Wu, T. Review on Optimal Scheduling of Integrated Energy Systems. *Power Syst. Technol.* **2021**, *45*, 2256–2272. [[CrossRef](#)]
- Zeng, M.; Liu, Y.; Zhou, P.; Wang, Y.; Hou, M. Review and Prospects of Integrated Energy System Modeling and Benefit Evaluation. *Power Syst. Technol.* **2018**, *42*, 1697–1708. [[CrossRef](#)]
- Chen, B.; Sun, H.; Chen, Y.; Guo, Q.; Wu, W.; Qiao, Z. Energy Circuit Theory of Integrated Energy System Analysis (I): Gaseous Circuit. *Proc. CSEE* **2020**, *40*, 436–444. [[CrossRef](#)]
- Chen, B.; Sun, H.; Yin, G.; Wu, W.; Guo, Q.; Chen, Y.; Pan, Z.; Wang, B. Energy Circuit Theory of Integrated Energy System Analysis (II): Hydraulic Circuit and Thermal Circuit. *Proc. CSEE* **2020**, *40*, 2133–2142, 2393. [[CrossRef](#)]
- Chen, B.; Sun, H.; Wu, W.; Guo, Q.; Qiao, Z. Energy Circuit Theory of Integrated Energy System Analysis (III): Steady and Dynamic Energy Flow Calculation. *Proc. CSEE* **2020**, *40*, 4820–4831. [[CrossRef](#)]
- Yin, G.; Chen, B.; Sun, H.; Guo, Q. Energy Circuit Theory of Integrated Energy System Analysis (IV): Dynamic State Estimation of the Natural Gas Network. *Proc. CSEE* **2020**, *40*, 5827–5837. [[CrossRef](#)]
- Chen, Y.; Sun, H.; Guo, Q. Energy Circuit Theory of Integrated Energy System Analysis (V): Integrated Electricity-Heat-Gas Dispatch. *Proc. CSEE* **2020**, *40*, 7928–7937+8230. [[CrossRef](#)]
- Geidl, M.; Koepfel, G.; Favre-Perrod, P.; Klockl, B.; Andersson, G.; Frohlich, K. Energy Hubs for the Future. *IEEE Power Energy Mag.* **2007**, *5*, 24–30. [[CrossRef](#)]
- Wang, Y.; Zhang, N.; Kang, C.; Kirschen, D.S.; Yang, J.; Xia, Q. Standardized Matrix Modeling of Multiple Energy Systems. *IEEE Trans. Smart Grid* **2019**, *10*, 257–270. [[CrossRef](#)]
- Liu, T.; Zhang, D.; Wang, S.; Wu, T. Standardized modelling and economic optimization of multi-carrier energy systems considering energy storage and demand response. *Energy Convers. Manag.* **2019**, *182*, 126–142. [[CrossRef](#)]
- Bloess, A. Modeling of combined heat and power generation in the context of increasing renewable energy penetration. *Appl. Energy* **2020**, *267*, 114727. [[CrossRef](#)]
- Wang, H.; Yang, J.; Chen, Z.; Li, G.; Liang, J.; Ma, Y.; Dong, H.; Ji, H.; Feng, J. Optimal dispatch based on prediction of distributed electric heating storages in combined electricity and heat networks. *Appl. Energy* **2020**, *267*, 114879. [[CrossRef](#)]
- Zhao, H.; Lu, H.; Wang, X.; Li, B.; Wang, Y.; Liu, P.; Ma, Z. Research on Comprehensive Value of Electrical Energy Storage in CCHP Microgrid with Renewable Energy Based on Robust Optimization. *Energies* **2020**, *13*, 6526. [[CrossRef](#)]
- Alotaibi, M.A.; Eltamaly, A.M. A Smart Strategy for Sizing of Hybrid Renewable Energy System to Supply Remote Loads in Saudi Arabia. *Energies* **2021**, *14*, 7069. [[CrossRef](#)]

15. Alotaibi, M.A.; Eltamaly, A.M. Upgrading Conventional Power System for Accommodating Electric Vehicle through Demand Side Management and V2G Concepts. *Energies* **2022**, *15*, 6541. [[CrossRef](#)]
16. Dou, X.; Zhao, W.; Lang, Y.; Li, Y.; Gao, C. A Review of Operation of Natural Gas-Electricity Coupling System Considering Power-to-Gas Technology. *Power Syst. Technol.* **2019**, *43*, 165–173. [[CrossRef](#)]
17. Liu, J.; Sun, W.; Yan, J. Effect of P2G on Flexibility in Integrated Power-Natural Gas-Heating Energy Systems with Gas Storage. *Energies* **2021**, *14*, 196. [[CrossRef](#)]
18. Fambri, G.; Diaz-Londono, C.; Mazza, A.; Badami, M.; Sihvonen, T.; Weiss, R. Techno-economic analysis of Power-to-Gas plants in a gas and electricity distribution network system with high renewable energy penetration. *Appl. Energy* **2022**, *312*, 118743. [[CrossRef](#)]
19. Andrade, C.; Seloosse, S.; Maïzi, N. The role of power-to-gas in the integration of variable renewables. *Appl. Energy* **2022**, *313*, 118730. [[CrossRef](#)]
20. Sun, W.; Harrison, G.P.; Dodds, P.E. A multi-model method to assess the value of power-to-gas using excess renewable. *Int. J. Hydrog. Energy* **2022**, *47*, 9103–9114. [[CrossRef](#)]
21. Cui, Y.; Yan, S.; Zhong, W.; Wang, Z.; Zhang, P.; Zhao, Y. Optimal Thermoelectric Dispatching of Regional Integrated Energy System with Power-to-Gas. *Power Syst. Technol.* **2020**, *44*, 4254–4264. [[CrossRef](#)]
22. Liu, Z.; Liu, R.; Liang, N.; Liu, X. Day-Ahead Optimal Economic Dispatching Strategy for Micro Energy-Grid with P2G. *Trans. China Electrotech. Soc.* **2020**, *35*, 535–543. [[CrossRef](#)]
23. Li, L.; Wang, J.; Zhong, X.; Lin, J.; Wu, N.; Zhang, Z.; Meng, C.; Wang, X.; Shah, N.; Brandon, N.; et al. Combined multi-objective optimization and agent-based modeling for a 100% renewable island energy system considering power-to-gas technology and extreme weather conditions. *Appl. Energy* **2022**, *308*, 118376. [[CrossRef](#)]
24. Li, P.; Wu, D.; Li, Y.; Liu, H.; Wang, N.; Zhou, X. Optimal Dispatch of Multi-Microgrids Integrated Energy System Based on Integrated Demand Response and Stackelberg game. *Proc. CSEE* **2021**, *41*, 1307–1321+1538. [[CrossRef](#)]
25. Luo, P.; Zhou, H.; Xu, L.; Lü, Q.; Wu, Q. Day-ahead Optimal Scheduling of Multi-microgrids with Combined Cooling, Heating and Power Based on Interval Optimization. *Autom. Electr. Power Syst.* **2022**, *46*, 137–146.
26. Zhou, X.; Han, X.; Li, T.; Wei, B.; Li, Y. Master-Slave Game Optimal Scheduling Strategy for Multi-Agent Integrated Energy System Based on Demand Response and Power Interaction. *Power Syst. Technol.* **2022**, *46*, 3333–3346. [[CrossRef](#)]
27. Guo, Y.; Wang, C.; Shi, Y.; Guo, C.; Shang, J.; Yang, X. Comprehensive Optimization Configuration of Electric and Thermal Cloud Energy Storage in Regional Integrated Energy System. *Power Syst. Technol.* **2020**, *44*, 1611–1623. [[CrossRef](#)]
28. Yan, M.; Li, H.; Wang, J.; He, Y. Optimal operation model of a park integrated energy system considering uncertainty of integrated demand response. *Power Syst. Prot. Control.* **2022**, *50*, 163–175. [[CrossRef](#)]
29. Zhao, H.; Miao, S.; Li, C.; Zhang, D.; Tu, Q. Research on Optimal Operation Strategy for Park-Level Integrated Energy System Considering Cold-Heat-Electric Demand Coupling Response Characteristics. *Proc. CSEE* **2022**, *42*, 573–589. [[CrossRef](#)]